Polymer Chemistry

ROYAL SOCIETY OF CHEMISTRY

COMMUNICATION

View Article Online
View Journal | View Issue

Cite this: *Polym. Chem.*, 2023, **14**, 2592

Received 7th April 2023,
Accepted 1st May 2023

DOI: 10.1039/d3py00379e

rsc.li/polymers

RAFT step-growth polymerization of bis-acrylamides and their facile degradation†

Parker T. Boeck, [a,c] Joji Tanaka, [b] Wei You, *[b] Brent S. Sumerlin *[a] and Adam S. Veige *[c]

Demonstrated is the successful $A_2 + B_2$ RAFT step-growth polymerization of bis-acrylamides using a bifunctional trithiocarbonate chain transfer agent as the comonomer. Remarkably, homopropagation typical of acrylamides leading to branching and crosslinking was not observed. Moreover, synthesized poly(acrylamides) can be degraded by simply adding excess ethanolamine or PBu_3.

Reversible addition–fragmentation chain transfer polymerization (RAFT) is a popular technique due to its user-friendly nature, vast functional group tolerance, excellent molecular weight and end group control, and the narrow dispersity of the resulting polymers.[1–7] RAFT is a reliable technique for the general practitioner to synthesize simple polymers, but more complex macromolecular architectures are also accessible.[8–11] One limitation of RAFT and other traditional controlled polymerizations of vinyl monomers is they produce degradation-resistant polymers with intractable C–C backbones. Expanding areas of research such as polymer recycling, biomedical applications, and tissue engineering are driving the search for alternative techniques for producing backbone degradable polymers.[12–19] Step-growth polymerization, in contrast, often requires harsh conditions leading to significantly decreased functional group tolerance.[20–22] Step-growth polymerizations traditionally produce mainchain polyesters and polyamides but high conversion again requires harsh conditions, and building complex architectures can be challenging.[23]

RAFT step-growth polymerization (or RAFT polyaddition according to IUPAC nomenclature) is a hybrid methodology that produces main-chain-functional linear polymers by repeated single-unit monomer insertion (SUMI) between stoichiometric amounts of chain transfer agent (CTA) and vinylic monomer. Importantly, it combines the key benefits of controlled radical polymerization (functional group tolerance, mild conditions, and ease of use) and step-growth polymerizations (backbone functionality). Tanaka *et al.* demonstrated the thermally initiated A_2 + B_2 and AB RAFT step-growth polymerization of maleimides and trithiocarbonate-based chain transfer agents (CTA).[24] By combining a bifunctional trithiocarbonate chain transfer agent, CTA_2 (Scheme 1A), and a bis-maleimide, then heating them in the presence of AIBN, RAFT step-growth polymerization was achieved for the first time. It is important to remember that the mechanism of propagation of RAFT step-growth polymerization is SUMI.[25–27] Maleimides, selected as the original target monomer, have low rates of homopropagation, thus decreasing the competition

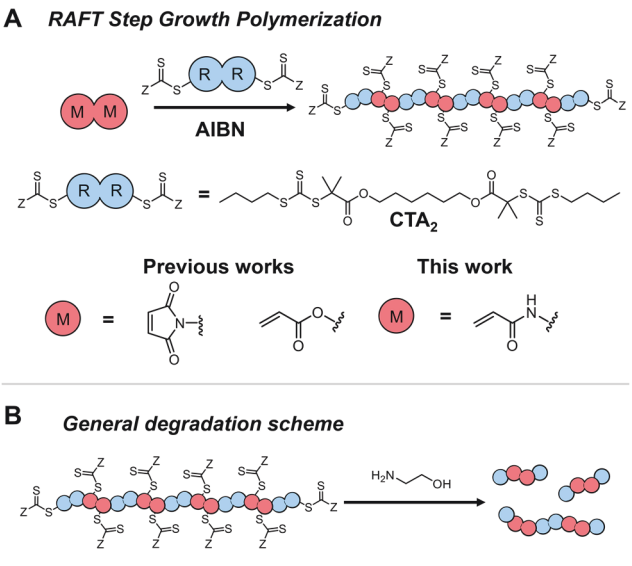

Scheme 1 General scheme of RAFT step-growth polymerization of CTA_2 (A) and bifunctional monomer and subsequent degradation using ethanolamine (B).

[a]*George & Josephine Butler Polymer Research Laboratory, Center for Macromolecular Sciences & Engineering, Department of Chemistry, University of Florida, P.O. Box 117200, Gainesville, Florida 32611, USA. E-mail: sumerlin@chem.ufl.edu*
[b]*Department of Chemistry, University of North Carolina at Chapel Hill, Chapel Hill, NC, 27599-3290, USA. E-mail: wyou@unc.edu*
[c]*Center for Catalysis, Department of Chemistry, University of Florida, P.O. Box 117200, Gainesville, Florida 32611, USA. E-mail: veige@chem.ufl.edu*
†Electronic supplementary information (ESI) available. See DOI: https://doi.org/10.1039/d3py00379e

between homopolymerization and trithiocarbonate addition (SUMI). Ensuring an efficient RAFT step-growth polymerization free of crosslinking and branching.[28,29] Shortly after, the Zhu group reported the A_2 + B_2 and AB light-induced RAFT step-growth polymerization of vinyl ethers and xanthates.[30] Notably, this enabled both cationic and radical grafting-from polymerization.

Recently, You *et al.* disclosed the successful thermal RAFT step-growth polymerization of bis-acrylates utilizing the same bifunctional trithiocarbonate CTA_2.[31] This was significant because maleimides and vinyl ethers do not homopolymerize rapidly, whereas acrylates undergo rapid homopolymerization with trithiocarbonate based CTA, thus an extremely efficient SUMI must be achieved to ensure a successful RAFT step-growth polymerization free of acrylate homopropagation which will lead to branching and/or crosslinking. Highlighting the utility of this technique to prepare degradable bottle-brush polymers, the successful incorporation of degradable disulfide bonds was achieved using a custom CTA. However, slow homopropagating monomers such as bis-maleimides, bis-ethers, and bis-olefins limit the scope of this exciting technique.[30,32,33] Like acrylates, acrylamides tend to undergo rapid homopolymerization in typical RAFT conditions with CTAs.[34,35] Given the ability of CTA_2 to effectively facilitate the RAFT step-growth polymerization of bis-acrylates we hypothesized bis-acrylamides would also be applicable, extending this method to the synthesis of polyamides. Further expanding the scope of RAFT step-growth polymerization, the A_2 + B_2 RAFT step-growth polymerization of a series of commercially available bis-acrylamides with CTA_2 is now achieved. Again, homopropagation of the bifunctional vinylic monomer was suppressed, leading to entirely linear RAFT step-growth polymers.

It is vital to match the CTA R group reactivity to any given monomer to ensure efficient SUMI and avoid vinylic monomer homopropagation.[26,27,36] BDMAT, the monofunctional equivalent of CTA_2 was tested for compatibility with acrylamides by combining DMA and BDMAT in a 1 : 1 ratio in dioxane with AIBN at 70 °C. A ^{1}H NMR spectrum of the reaction mixture indicated the consumption of DMA and the appearance of the RAFT-SUMI product (Fig. S1†). Gratifyingly, the yield (94% after 12 h) of RAFT-SUMI product increased proportionally with the loss of DMA (Fig. 1 and Table S1†). Satisfied that BDMAT facilitates SUMI of acrylamides the next attempt was to initiate A_2 + B_2 RAFT step-growth polymerization with a bifunctional equivalent of BDMAT (CTA_2) and a series of commercially available bis-acrylamides.

Attempting RAFT step-growth polymerization of *N*,*N*′-piperazinebis(acrylamide) (PBA) with CTA_2 for the first time, the reagents were combined in dioxane and initiated with AIBN at 70 °C to produce **P(MBA-*alt*-CTA$_2$)** (Fig. 2A). Monitoring the reaction progress is possible by measuring the disappearance of the acrylamide vinyl peak at ~5.7 ppm relative to the CH_3-protons of the Z group while simultaneously monitoring molecular weight *via* GPC. (Fig. S2–S12†). Some low molecular weight oligomers overlap with the solvent likely leading to

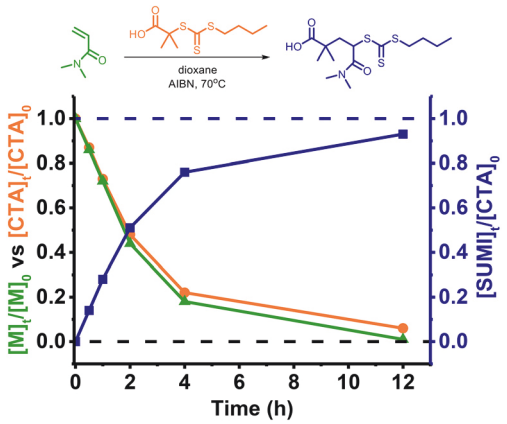

Fig. 1 Plot of AIBN initiated model SUMI reaction of DMA with BDMAT. DMA and BDMAT conversion as well as RAFT-SUMI product yield were measured *via* ^{1}H NMR spectroscopy.

overestimation of the molecular weight at low conversions (Fig. S3†). Gratifyingly, an exponential-like increase of number-average (M_n), weight-average (M_w) and Z-average (M_z) molecular weight with increasing acrylamide conversion (p), was observed, as expected for a step-growth polymerization (Fig. 2A). Flory derived equations (eqn (S1)–(S3)†) that describe the increase of M_n, M_w, and M_z with increasing monomer conversion for an ideal step-growth polymerization based on the structural molecular weight (M_0).[37] Experimentally measured molecular weight data correlate with plots of the Flory functions (Fig. 2A). These observations are consistent with thermally initiated RAFT step-growth polymerization with CTA_2.

The RAFT step-growth polymerization of secondary bis-acrylamides was explored next. Given the insolubility of acrylamides (owing to their ability to hydrogen bond) in dioxane and other common organic solvents, *m*-cresol was selected as the polymerization solvent. RAFT step-growth polymerization of *N*,*N*′-methylenebis(acrylamide) (MBA), the simplest bis-acrylamide, with CTA_2 yields an exponential-like molecular weight increase characteristic of a step growth polymerization (Fig. 2B). The polymerization consumes 97% of the monomer in only 4 h and generates a polymer with a M_w of 16 000 (Table 1). Using a published equation, it is possible to calculate the corrected instantaneous weight-average molecular weight ($M_{w,th}(r_{th})$) by estimating the stoichiometric imbalance (r_{th}) induced by AIBN initiation of the polymerization at 70 °C at a given time t.[24,32] The crude polymer M_w of 16k more closely matches the corrected theoretical molecular weight of 13k, $M_{w,th}(r_{th,AIBN})$, than the 24k $M_{w,thr}$ predicted by Flory's original equations (Table 1). Flory's equation assumes a stoichiometric balance of reacting functional groups for an ideal step-growth polymerization and does not account for irreversible cyclization during polymerization.[37] While $M_{w,th}(r_{th})$ accounts for initiation it neglects radical termination and assumes a constant initiator efficiency (f = 0.65) which may lead to overestimation of the imbalance at extended reaction times.

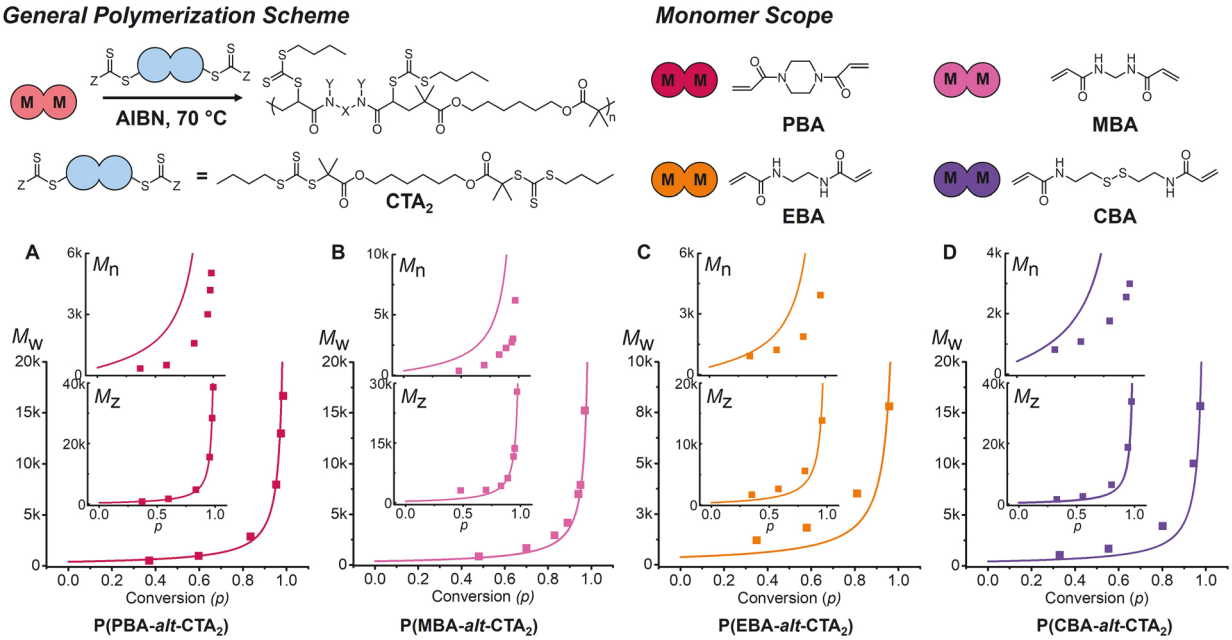

Fig. 2 Experimentally measured (■) and theoretically predicted (eqn (S1)–(S3)†) molecular weight evolution of the RAFT step-growth polymerization of CTA_2 and various commercially available secondary bis-acrylamides (A–D). Experimental molecular weight averages (M_n, M_w and M_z) were measured by conventional GPC analysis (DMAc, 50 °C, dRI detection) against PMMA standards.

Table 1 Polymerization and characterization of CTA_2 and bis-acrylamide derived RAFT step-growth polymers

Entry	Polymer	Time[a] (h)	Conv. (p)[b]	$M_{w,th}$ [c]	$M_{w,th}(r_{th})$ [d]	$M_{w,crude}$ [e]	$M_{w,isol.}$ [e]	$Đ_{isol.}$ [e]	a [f]	T_g [g] (°C)	T_{95} [h] (°C)
1	**P(PBA-*alt*-CTA$_2$)**	8	98	48k	14k	17k	19k	2.1	0.645	14	240
2	**P(MBA-*alt*-CTA$_2$)**	4	97	24k	13k	15k	16k	1.6	0.715	17	237
3	**P(EBA-*alt*-CTA$_2$)**	4	96	18k	11k	8k	11k	1.3	1.031	16	234
4	**P(CBA-*alt*-CTA$_2$)**	6	98	33k	14k	16k	20k	1.9	0.703	11	239

[a] Duration of respective polymerization. [b] Bis-acrylamide conversion measured by ^{1}H-NMR spectroscopy. [c] Theoretical weight-average molecular weight using Flory's equation for an ideal step-growth polymerization (eqn (S1)–(S3)†). [d] Theoretical weight-average molecular weight considering initiator derived imbalanced stoichiometry. [e] Weight-average molecular weight and dispersity ($Đ$) measured by conventional GPC analysis (DMAc, 50 °C, dRI detection) using PMMA standards. [f] Exponent parameter (a) of Mark–Houwink–Sakurada plot measured by GPC analysis in THF. [g] Glass transition temperature (T_g) measured by DSC. [h] Temperature at 5% mass loss (T_{95}) measured by TGA.

RAFT step-growth polymerization of *N*,*N*′-ethylenebis(acrylamide) (EBA), again reveals an exponential-like molecular weight evolution (Fig. 2C). EBA RAFT step-growth polymerization proceeds slowly and only reaches 96% conversion and a resulting polymer M_w of 11 000. Finally, RAFT step-growth polymerization of *N*,*N*′-cystaminebis(acrylamide) provides a high molecular weight polymer in 6 h with an exponential-like molecular weight evolution (Table 1 and Fig. 2D). Data supporting the structural assignment of all synthesized RAFT step-growth polymers comes from ^{1}H NMR and ^{13}C NMR spectroscopy (Fig. S13–S20†). In all cases the data supports polymer compositions free of homopropagation and marks the first use of this protocol to initiate RAFT step-growth polymerization of both secondary and tertiary bis-acrylamides.

Thermogravimetric analysis (TGA) and differential scanning calorimetry (DSC) (Fig. S26–S29†) were used to interrogate the thermal properties of the synthesized polymers. Attributable to thermolytic cleavage of Z group side chains, the data reveal a two-step thermal decomposition profile (Fig. S30–S33†).[32,38,39] In fact, all four polymers demonstrate similar T_{95} values in the range of 234–240 °C (Table 1). The polymers also exhibit similar glass transition temperatures, indicating their amorphous nature, with values ranging from 11–17 °C.

Using a multi-detector GPC equipped with a light-scattering and viscometer with THF as the eluent, the solution phase polymer conformation a-value was obtained from Mark–Houwink–Sakurada plots (MHS) of intrinsic viscosity as a function of molecular weight (Fig. S38†). Linear polymers exhibit an a value greater than 0.5, whereas dense architectures, such as branched polymers have an a less than 0.5.[40–42] Suggesting all four polymers are linear, the MHS plots reveal a-values greater than 0.5, again suggesting a lack of bis-acrylamide homopropagation (Table 1 and Fig. S38†). Although, **P(EBA-*alt*-CTA$_2$)** displayed an abnormally high a-value (1.031). This is

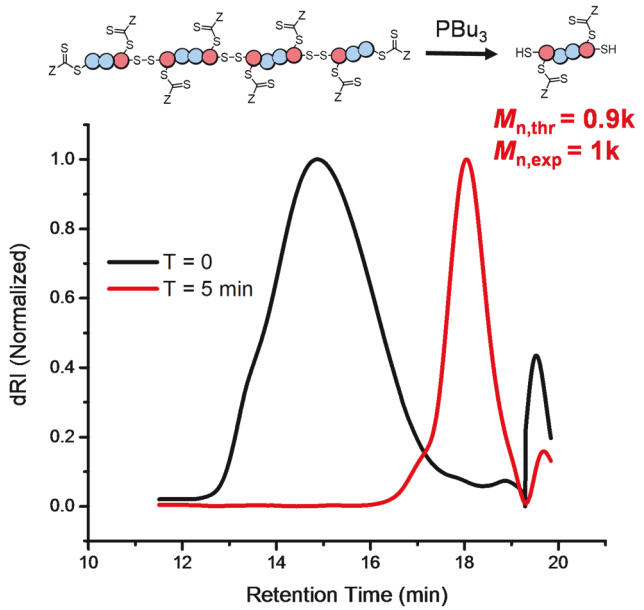

Fig. 3 GPC chromatogram (DMAc, 50 °C, dRI detection) of **P(CBA-*alt*-CTA$_2$)** before and after the addition of PBu$_3$.

consistent with previous literature reports that the Mark–Houwink–Sakurada plot can be inaccurate for polymers of a low molecular weight.[43]

One key benefit of RAFT step-growth polymerization is the ability to incorporate functional groups into the main-chain polymeric backbone. Previous, RAFT step-growth incorporating cleavable disulfide bond groups required the synthesis of a custom CTA. The results presented here are significant because the disulfide-containing CBA is commercially available, thus opening easy access to degradable polymers. **P(CBA-*alt*-CTA$_2$)** degrades in 5 min by simply adding PBu$_3$ in dioxane. Fig. 3 depicts the GPC traces of the polymer before and after addition of PBu$_3$. Clearly, the degraded products (M_n = 1000) match the expected cleaved monomer unit (M_n = 900). Yet, inherently this degradation is specific to only **P(CBA-*alt*-CTA$_2$)**.

RAFT step-growth polymerization with CTA$_2$ places an ester in the polymer backbone. A degradation that targets this common weak link is more desirable. Surprisingly, **P(MBA-*alt*-CTA$_2$)** degrades in 2 h after addition of ethanolamine. Fig. 4A and B shows GPC traces (dRI and UV-Vis detection) of **P(MBA-*alt*-CTA$_2$)** before and after the addition of ethanolamine. Clearly, full Z group removal occurs within 20 min, confirmed by a lack of absorbance at 308 nm, but dRI detection demonstrated continued mass loss after 20 min suggesting backbone degradation of **P(MBA-*alt*-CTA$_2$)**. The GPC traces exhibit some

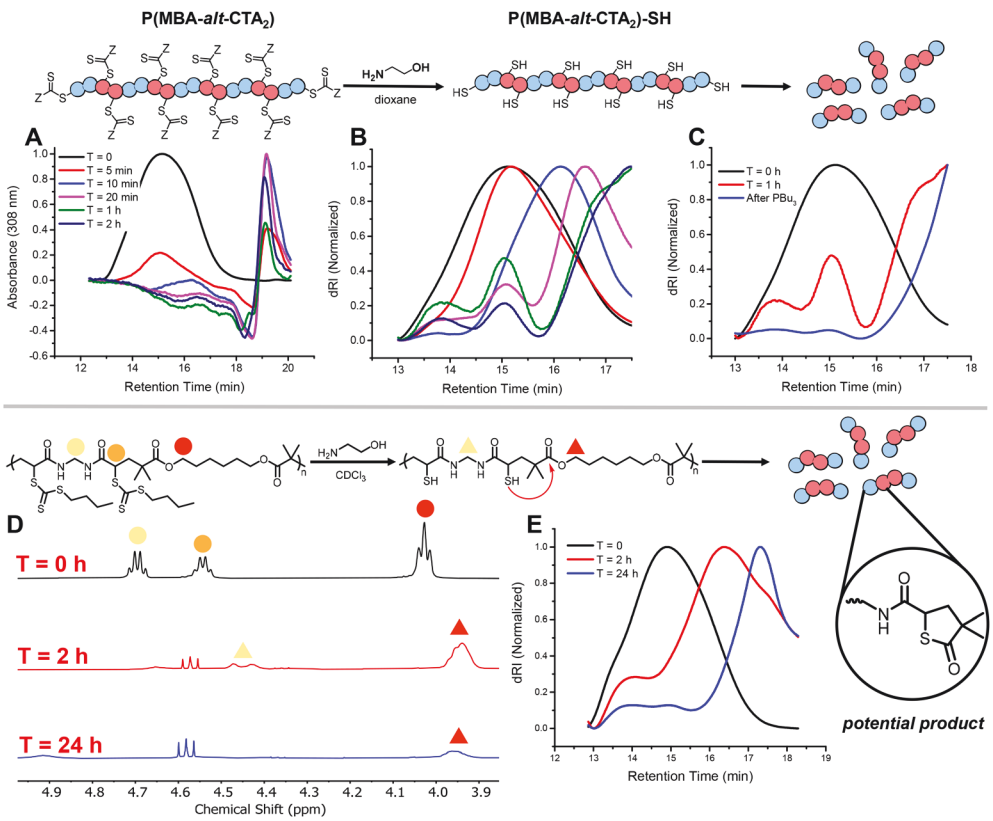

Fig. 4 GPC chromatograms (DMAc, 50 °C, dRI/UV-Vis detection) before and after the addition of ethanolamine to **P(MBA-*alt*-CTA$_2$)** (A and B) followed by the addition of PBu$_3$ after 2 h (C). Concurrent ^{1}H NMR and GPC analysis before and after the addition of ethanolamine to **P(MBA-*alt*-CTA$_2$)** in CDCl$_3$ (D and E).

higher molecular weight products. Oxidative coupling between cleaved oligomer thiols, previously documented during trithiocarbonate aminolysis,[44,45] explains the observed higher molecular weight products. Supporting the hypothesis of oxidative coupling, adding PBu_3 to the mixture cleaves these units as can be seen in the blue trace within Fig. 4C. Additional evidence that backbone degradation followed Z-group cleavage comes from concurrent ^{1}H NMR spectroscopy and GPC analysis of the reaction in $CDCl_3$. Full Z-group cleavage occurs at 2 h, confirmed by the disappearance of the methine proton adjacent to the Z group in Fig. 4D. Continued mass loss, indicative of backbone degradation, was observed after 2 h (Fig. 4E). Unfortunately, characterization of the degradation products proved difficult, thus precluding elucidation of the active mechanism. However, one proposal is that degradation proceeds first through cleavage of the Z group by ethanolamine, furnishing thiol-terminated products **P(MBA-*alt*-CTA$_2$)-SH**, as confirmed by ^{1}H NMR spectroscopy (Fig. S40†). Thiolactonization of the adjacent ester could then cleave the backbone. Indeed, there is literature precedent for thiolactonization following Z group aminolysis, though such a mechanism resulting in polymer degradation is unprecedented.[46] The presence of significantly downfield (195+ ppm) carbon NMR resonances similar to values previously reported for thiolactones bearing electron-withdrawing groups is consistent with the presence of thiolactone (Fig. S42†).[47,48]

Thiolactonization, according to Fig. 4 requires the thiol to be in proximity to the ester in the backbone. Increasing the distance of the thiol from the ester should prevent degradation by the mechanism proposed above. Using 4-acryloylmorpholine, grafting-from polymerization was performed on **P(BM-*alt*-CTA$_2$)** to afford **PBM-*alt*-CTA$_2$-*graft*-P(NAM)**. Adding ethanolamine to **PBM-*alt*-CTA$_2$-*graft*-P(NAM)** in dioxane yielded the thiol terminated brush, **PBM-*alt*-CTA$_2$-*graft*-P(NAM)-SH**. UV-Vis and ^{1}H NMR spectra of the precipitated product confirms the trithiocarbonate was cleaved (Fig. S43 and S44†). Fig. 5 depicts the GPC spectra before and after the addition of ethanolamine to **PBM-*alt*-CTA$_2$-*graft*-P(NAM)**. Obvious from the GPC traces is that no mass loss occurs, offering support for the hypothesis that degradation occurs *via* thiolactonization.

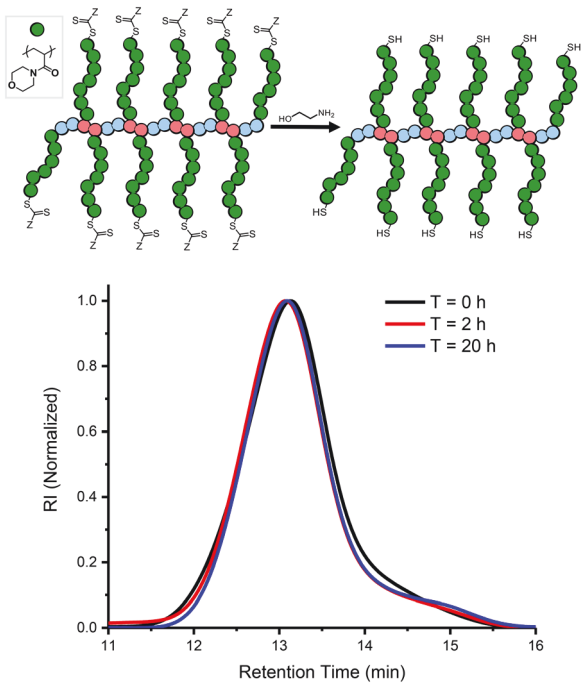

Fig. 5 GPC chromatograms (DMAc, 50 °C, dRI detection) before and after addition of ethanolamine to **PBM-*alt*-CTA$_2$-P(NAM)**.

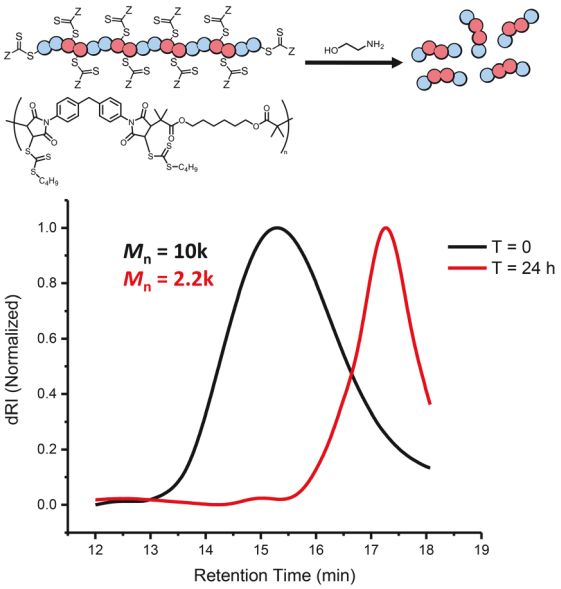

Fig. 6 GPC chromatogram (DMAc, 50 °C, dRI detection) of **P(BM-*alt*-CTA$_2$)** before and after the addition of excess ethanolamine.

Presumably, degrading other polymers derived from RAFT step-growth using CTA_2 is also possible. **P(BM-*alt*-CTA$_2$)**,[32] synthesized according to previously reported methods, also degrades easily by simply adding ethanolamine. Fig. 6 depicts the GPC trace before and after the addition of ethanolamine to **P(BM-*alt*-CTA$_2$)**. The low molecular weight (M_n = 2200) of the products confirms backbone cleavage of the polymer.

In summary, RAFT step-growth polymerization of both tertiary and secondary acrylamides using CTA_2 was demonstrated for the first time. Chromatographic and spectroscopic interrogation of the polymerization confirms the mechanism of propagation. MHS and NMR data supports the claim of negligible homopropagation during polymerization leading to linear polymers. In addition, a generalizable degradation mechanism for RAFT step-growth polymers derived from CTA_2 was discovered.

Author contributions

P. T. B. and J. T. conceptualized the study. P. T. B. drafted the manuscript. P. T. B. and J. T. collected and curated data. P. T.

B, J. T., W. Y., B. S. S., and A. S. V. revised the manuscript. A. S. V. and B. S. S. supervised the work.

Conflicts of interest

The authors declare the following competing financial interest (s): J. T. and W. Y. are named inventors on the provisional patent application described in this work.

Acknowledgements

This material is based upon work supported by the National Science Foundation, CHE-2108266 (UF) and CHE-2108670 (UNC).

References

1 J. Chiefari, Y. K. Chong, F. Ercole, J. Krstina, J. Jeffery, T. P. T. Le, R. T. A. Mayadunne, G. F. Meijs, C. L. Moad, G. Moad, E. Rizzardo and S. H. Thang, *Macromolecules*, 1998, **31**, 5559–5562.
2 G. Moad, E. Rizzardo and S. H. Thang, *Aust. J. Chem.*, 2009, **62**, 1402–1472.
3 M. R. Hill, R. N. Carmean and B. S. Sumerlin, *Macromolecules*, 2015, **48**, 5459–5469.
4 T. Kubo, J. L. Swartz, G. M. Scheutz and B. S. Sumerlin, *Macromol. Rapid Commun.*, 2019, **40**, 1–5.
5 C. P. Easterling, C. P. Easterling, G. Coste, J. E. Sanchez, G. E. Fanucci and B. S. Sumerlin, *Polym. Chem.*, 2020, **11**, 2955–2958.
6 G. Moad, E. Rizzardo and S. H. Thang, *Aust. J. Chem.*, 2012, **65**, 985–1076.
7 S. Perrier, *Macromolecules*, 2017, **50**, 7433–7447.
8 J. Rosselgong, E. G. L. Williams, T. P. Le, F. Grusche, T. M. Hinton, M. Tizard, P. Gunatillake and S. H. Thang, *Macromolecules*, 2013, **46**, 9181–9188.
9 J. Tanaka, S. Häkkinen, P. T. Boeck, Y. Cong, S. Perrier, S. S. Sheiko and W. You, *Angew. Chem., Int. Ed.*, 2020, **132**, 7270–7275.
10 C. Zhang, Y. Zhou, Q. Liu, S. Li, S. Perrier and Y. Zhao, *Macromolecules*, 2011, **44**, 2034–2049.
11 J. Zhao, Y. Zhou, Y. Zhou, N. Zhou, X. Pan, Z. Zhang and X. Zhu, *Polym. Chem.*, 2016, **7**, 1782–1791.
12 M. Hong and E. Y. X. Chen, *Green Chem.*, 2017, **19**, 3692–3706.
13 T. Thanh, H. Thi, E. H. Pilkington, D. H. Nguyen and J. S. Lee, *Polymers*, 2020, **12**, 298.
14 O. Ivanchenko, U. Authesserre, G. Coste, S. Mazières, M. Destarac and S. Harrisson, *Polym. Chem.*, 2021, **12**, 1931–1938.
15 T. Endo and F. Sanda, *J. Polym. Sci., Part A: Polym. Chem.*, 2001, **39**, 265–276.
16 M. R. Hill, T. Kubo, S. L. Goodrich, C. A. Figg and B. S. Sumerlin, *Macromolecules*, 2018, **51**, 5079–5084.
17 G. R. Kiel, D. J. Lundberg, E. Prince, K. E. L. Husted, A. M. Johnson, V. Lensch, S. Li, P. Shieh and J. A. Johnson, *J. Am. Chem. Soc.*, 2022, **144**, 12979–12988.
18 R. A. Smith, G. Fu, O. McAteer, M. Xu and W. R. Gutekunst, *J. Am. Chem. Soc.*, 2019, **141**, 1446–1451.
19 G. G. Hedir, C. A. Bell, N. S. Ieong, E. Chapman, I. R. Collins, R. K. O'Reilly and A. P. Dove, *Macromolecules*, 2014, **47**, 2847–2852.
20 G. N. Short, H. T. H. Nguyen, P. I. Scheurle and S. A. Miller, *Polym. Chem.*, 2018, **9**, 4113–4119.
21 P. Qi, H. L. Chen, H. T. H. Nguyen, C. C. Lin and S. A. Miller, *Green Chem.*, 2016, **18**, 4170–4175.
22 O. Nsengiyumva and S. A. Miller, *Green Chem.*, 2019, **21**, 973–978.
23 H. Carothers, *Trans. Faraday Soc.*, 1936, **32**, 39–49.
24 J. Tanaka, N. E. Archer, M. J. Grant and W. You, *J. Am. Chem. Soc.*, 2021, **143**, 15918–15923.
25 J. Xu, *Macromolecules*, 2019, **52**, 9068–9093.
26 J. Xu, C. Fu, S. Shanmugam, C. J. Hawker, G. Moad and C. Boyer, *Angew. Chem., Int. Ed.*, 2017, **56**, 8376–8383.
27 J. Xu, S. Shanmugam, C. Fu, K. F. Aguey-Zinsou and C. Boyer, *J. Am. Chem. Soc.*, 2016, **138**, 3094–3106.
28 S. Pfeifer and J. F. Lutz, *J. Am. Chem. Soc.*, 2007, **129**, 9542–9543.
29 G. Deng and Y. Chen, *Macromolecules*, 2004, **37**, 18–26.
30 Z. Li, J. Li, X. Pan, Z. Zhang and J. Zhu, *ACS Macro Lett.*, 2022, **11**, 230–235.
31 N. E. Archer, P. T. Boeck, Y. Ajirniar, J. Tanaka and W. You, *ACS Macro Lett.*, 2022, **11**, 1079–1084.
32 P. T. Boeck, N. E. Archer, J. Tanaka and W. You, *Polym. Chem.*, 2022, **13**, 2589–2594.
33 Z. Li, J. Li, B. Zhao, X. Pan, X. Pan and J. Zhu, *Chin. J. Chem.*, 2022, **41**, 503–508.
34 R. N. Carmean, T. E. Becker, M. B. Sims and B. S. Sumerlin, *Chem*, 2017, **2**, 93–101.
35 C. A. Figg, J. D. Hickman, G. M. Scheutz, S. Shanmugam, R. N. Carmean, B. S. Tucker, C. Boyer and B. S. Sumerlin, *Macromolecules*, 2018, **51**, 1370–1376.
36 D. J. Keddie, G. Moad, E. Rizzardo and S. H. Thang, *Macromolecules*, 2012, **45**, 5321–5342.
37 P. J. Flory, *J. Am. Chem. Soc.*, 1936, **58**, 1877–1885.
38 A. Postma, T. P. Davis, G. Moad and M. S. O'Shea, *Macromolecules*, 2005, **38**, 5371–5374.
39 T. Legge, A. Slark and S. Perrier, *J. Polym. Sci., Part A: Polym. Chem.*, 2006, **44**, 6980–6987.
40 A. B. Cook, R. Barbey, J. A. Burns and S. Perrier, *Macromolecules*, 2016, **49**, 1296–1304.
41 Y. Lu, L. An and Z. G. Wang, *Macromolecules*, 2013, **46**, 5731–5740.
42 A. P. Vogt and B. S. Sumerlin, *Macromolecules*, 2008, **41**, 7368–7373.
43 H. G. Barth and J. W. Mays, *Modern Methods of Polymer Characterization*, Wiley, New York, 1st edn, 1991.
44 D. L. Patton, M. Mullings, T. Fulghum and R. C. Advincula, *Macromolecules*, 2005, **38**, 8597–8602.

45 V. Lima, X. Jiang, J. Brokken-Zijp, P. J. Schoenmakers, B. Klumperman and R. Van Der Linde, *J. Polym. Sci., Part A: Polym. Chem.*, 2005, **43**, 959–973.
46 J. Xu, J. He, D. Fan, X. Wang and Y. Yang, *Macromolecules*, 2006, **39**, 8616–8624.
47 I. Suzuki, Y. Sakamoto, Y. Seo, Y. Ninomaru, K. Tokuda and I. Shibata, *J. Org. Chem.*, 2020, **85**, 2759–2769.
48 G. Wang, J. Li and Y. Xu, *Org. Biomol. Chem.*, 2008, **6**, 2995–2999.